frontiers | Frontiers in Materials

ORIGINAL RESEARCH
published: 26 September 2022
doi: 10.3389/fmats.2022.944274

Enhanced Carboxymethylcellulose Sponge for Hemostasis and Wound Repair

Zhanjian Bi[1], *Haifeng Teng*[1], *Qiujing Li*[2] *and Shukun Zhang*[2]*

[1]Intensive Care Unit, Weihai Municipal Hospital, Cheeloo College of Medicine, Shandong University, Weihai, China, [2]Department of Pathology, Weihai Municipal Hospital, Cheeloo College of Medicine, Shandong University, Weihai, China

Skin is the interface between human beings and the outside world. After skin injury, bleeding control and wound protection is urgently needed. In the study, the carboxymethyl cellulose/carboxymethyl chitosan-polydopamine (CMC/CMCS-PDA) sponge is prepared for skin hemostasis and repair. The self-polymerization of dopamine (DA) and cross-linking between DA and CMCS are simultaneously completed by Michael addition reaction to form CMCS-PDA under alkaline conditions. CMCS-PDA is introduced into the CMC sponge by EDC/NHS to improve the hemostasis ability and wound repair. By increasing the dosage of CMCS to get CMC/CMCS-PDA$_1$, CMC/CMCS-PDA$_2$, and CMC/CMCS-PDA$_3$ sponges, and the stability of CMC/CMCS-PDA sponge is improved with the increasing addition of CMCS. Compared with a simple CMC/PDA sponge, CMC/CMCS-PDA sponge has a high hemostatic effect for its dispersion stability and CMC/CMCS-PDA2 exhibits the best hemostatic ability with proper crosslinking. At the same time, the prepared CMC/CMCS-PDA sponge has good antibacterial and antioxidant properties. Rat skin wound model showed that CMC/CMCS-PDA sponge can better promote wound repair. Therefore, CMC/CMCS-PDA sponge could be a potential wound dressing for skin hemostasis and repair.

Keywords: carboxymethylcellulose, dopamine, carboxymethyl chitosan, skin, wound healing

OPEN ACCESS

Edited by:
Alessia Longoni,
University of Otago, New Zealand

Reviewed by:
Vaneet Kumar,
CT Group Of Institutions, Jalandhar, India
Chandra Srivastava,
Amity University Gurgaon, India
Diego Velasco,
Universidad Carlos III de Madrid de Madrid, Spain

***Correspondence:**
Shukun Zhang
zhangshukun0475@126.com

Specialty section:
This article was submitted to Biomaterials, a section of the journal Frontiers in Materials

Received: *15 May 2022*
Accepted: *15 June 2022*
Published: *26 September 2022*

Citation:
Bi Z, Teng H, Li Q and Zhang S (2022) Enhanced Carboxymethylcellulose Sponge for Hemostasis and Wound Repair. Front. Mater. 9:944274. doi: 10.3389/fmats.2022.944274

INTRODUCTION

Skin is the largest human organ, which can protect against the loss of fluids and nutrients (Buraczewska et al., 2007; Gurtner et al., 2008; Zhang et al., 2022). After an injury, the bleeding and fluid loss can slow down the recovery of wounds (Ong et al., 2008; Saporito et al., 2018; Ghomi et al., 2019). Therefore, skin wound dressings with hemostatic and water-retaining properties have potential application value in daily life.

Cellulose is the most widespread polysaccharide with good biocompatibility and water retention ability (Chang and Zhang, 2011; Halib et al., 2017; Saruchi and Kumar, 2020). Its development and utilization can bring high economic and medical value. Carboxymethyl cellulose (CMC) is the derivative of cellulose and has overcome the problem of solubility (Nelson et al., 1800; Pettignano et al., 2019; Zennifer et al., 2021). Sponges based on CMC have been widely used in wound dressings due to their advantages of low price and good water

retention ability (Eivazzadeh-Keihan et al., 2021; Diaz-Gomez et al., 2022; Ohta et al., 2022). In order to improve the stability of the CMC sponge, divalent ions and cross-linking agents are commonly used to cross-link CMC molecules (Liu et al., 2015; Kanikireddy et al., 2020; Pinpru and Woramongkolchai, 2020; Khalf-Alla et al., 2021). But the flexibility and chelating speed of divalent ions chelation are difficult to control. On this basis, suitable cross-linking agents are a good choice to crosslink CMC for improving the stability of the CMC sponge. Carboxymethyl chitosan (Upadhyaya et al., 2013; Lin et al., 2020; Wang et al., 2020) (CMCS) is a natural modified polysaccharide with rich functional groups. In addition, CMCS has good antibacterial properties and can regulate wound repair (Peng et al., 2011; Lin et al., 2020). Therefore, CMCS is an appropriate crosslink molecule for CMC.

Hemostasis is the first step of wound repair (Cheng et al., 2018a). Skin wound dressing with a rapid hemostasis effect can accelerate the process of wound repair (Park et al., 2018; Liang et al., 2021). Dopamine (DA) has attracted more and more attention in hemostasis and antioxidants for its catechin structure (Beck et al., 2004; Han et al., 2020; Li et al., 2020). DA can achieve oxidative autopolymerization to form PDA under alkaline conditions (Faure et al., 2013; Yang et al., 2014). Besides, DA can cross-link with the amino of polysaccharides (chitosan, carboxymethyl chitosan, gelatin, etc.) and finish polymerization on the surface of polysaccharides through the Michael addition reaction during the oxidation process (Felger and Miller, 2012; Qiu et al., 2018; Liu et al., 2021a). On this basis, dopamine can be introduced into CMCS through oxidative polymerization to form larger molecules of CMCS-PDA. CMC cross-linked by CMCS-PDA avoids the introduction of a large amount of cross-linking agents. The introduction of intermediate molecules to improve the stability of the CMC sponge has potential application value.

Therefore, in the study, DA polymerize and crosslink with CMCS to form a CMCS-PDA structure. CMC molecules are connected by CMCS-PDA with EDC/NHS to improve the stability of the CMC sponge. By adjusting the amount of CMCS, the degradation and hemostasis ability of sponges were studied. The colony formation method was adopted to study the growth inhibition effect of CMC/CMCS-PDA sponges to *S.aureus* and *E.coli*. The rapid hemostasis effect of CMC/CMCS-PDA sponges was evaluated in the rat liver injury model and rat tail severing experiment. Cytocompatibility experiments and skin incision model further explored the *in vitro* and *in vivo* biological properties of prepared sponges. Above, CMC/CMCS-PDA sponge could be a potential wound dressing for skin wound repair.

MATERIALS AND METHODS

Materials

Carboxymethyl cellulose (CMC, MW = 250,000, DS = 0.9), carboxymethyl chitosan (CMCS DS ≥ 80%, O-substituted), dopamine (DA), 1-ethyl-3-(3-dimethylaminopropyl) (EDC) and N-hydroxysuccinimide were obtained from Macklin' Co., Ltd.; CCK-8 kit was supported by Sigma-Aldrich Co., Ltd.; ABTS antioxidant kit, AO/EB staining reagents were purchased from Solarbio Co., Ltd.

Fabrication of CMC/CMCS-PDA Composite Polymer Sponge

Firstly, 0.3 g CMC was dissolved in 20 ml of deionized water. Then 0.05, 0.1, and 0.15 g CMCS were added into the above solution respectively and stirred to form a homogeneous solution. Next 10 mg DA was added to the homogeneous solution and the three groups were named CMC/CMCS-PDA_1, CMC/CMCS-PDA_2, and CMC/CMCS-PDA_3. Next, the pH of the above solution was adjusted to 8.5. After stirring in air for 2 h, the pH was adjusted to 6 and cooled at 4°C for 30 min. EDC/NHS (the molar ratio of EDC to NHS is 1:1 and the amount of crosslinking agent according to the amount of NH_2 in CMCS) was then added and stirred for 3 min. After that, the solution was transferred to a mold and placed at room temperature for 2 h to achieve reaction. Finally, the solution was frozen at −20°C and lyophilized to obtain CMC/CMCS-PDA sponges.

Fabrication of CMC/PDA Sponge

The CMC/PDA sponge is set as the control group. The preparation process is as follows: 0.3 g CMC was dissolved in 20 ml of deionized water. Then 10 mg DA was then added to the above solution and stirred to form a homogenous solution and the pH was adjusted to 8.5. After stirring in air for 2 h, the pH was adjusted to 6 and cooled at 4°C for 30 min. After that, EDC/NHS (the molar ratio of EDC to NHS is 1:1 and the amout of crosslinking agent is according to the amount of NH_2 in CMCS) was then added and reacted for 2 h. Next, the solution was transferred into a mold and frozen at −20°C. The CMC/PDA sponge was obtained after lyophilizing.

Surface Morphology and Chemical Composition Tests

Fourier transform infrared spectroscopy (FT-IR, Nicolet Nexus spectrometer) was used to detect the chemical composition of prepared sponges with the measurement range of 4000–400 cm^{-1}. The surface morphology of the sponge was studied by scanning electron microscope (SEM, JSM 6390, JEOL, Japan).

Water and Blood Absorption Test

The test process is as follows: the prepared sponge weighing W_1 was soaked in enough water and blood, respectively. After fully contacted, the sponge was taken out and the water and blood on the surface were cleared. The weight of the sponge was recorded as W_2. The water/blood absorption capacity (W) of the sponge was determined by the formula (2):

$$W = \frac{W_2 - W_1}{W_1} \times 100\% \quad (1)$$

W_2 and W_1 are the weight of sponges after and before water and blood absorption.

In vitro Degradation

The degradation was measured according to the previous method (Pei et al., 2015). The sponge weighing W_1 was placed in PBS (phosphate buffer solution) containing lysozyme (0.5 mg/ml), and the PBS was replaced every three days. The sponges were taken out and freeze-dried and weighed (W_2) at days 1, 3, 5, 7, and 14. Degradation rate (D) is calculated by **Eq. 3**:

$$D(\%) = \frac{W_1 - W_2}{W_1} \times 100\% \quad (2)$$

W_1 and W_2 were the initial and final weights of sponges respectively.

Antibacterial Properties Assay

Firstly, CMC/DA and CMC/CMCS-PDA sponges were sterilized under an ultraviolet lamp for 30 min 0.015 g sponge was added into a 5 ml liquid medium. *S. aureus* and *E. coli* were inoculated on the medium respectively and cultured in a 37°C shaker for 4 h. The absorbance of the bacterial solution was detected at 600 nm. The group without sponges was the blank group.

Free Radical Scavenging Test

The free radical scavenging capacity of the prepared sponge was tested through ABTS radical scavenging experiment. Firstly, 1 ml extraction and 10 mg sponge were added into a tube and bathed in 37°C water for 30 min. Following this, the tube was centrifuged at 10,000 rpm for 20 min and the supernatant was taken out for use. The supernatant was mixed with the ABTS kit as the experimental group and the supernatant was set as a control group. The mixed solution was incubated in a dark environment for 6 min and the absorbance was measured at 405 nm. The ABTS scavenging ability (*S*) was calculated by the formula (4):

$$S = \left[A_{\text{Blank}} - \left(A_{\text{Experiment}} - A_{\text{Control}}\right)\right] / A_{\text{Blank}} \times 100\% \quad (3)$$

A_{Blank} and A_{Control} are the absorbances of the blank group and control group respectively. $A_{\text{Experiment}}$ means the absorbance of a prepared sponge.

Hemolysis Assay

The Hemolysis rate test refers to the published literature (Cheng et al., 2018b). First, the anticoagulant rabbit blood was centrifuged until the supernatant was transparent. Erythrocytes were obtained by removing the supernatant and the erythrocytes were diluted to 5% with normal saline for use. Then, 2 ml diluted erythrocytes were added to the centrifuge tubes containing 10 mg sponge or gauze and incubated at 37°C for 1 h. Then the centrifuge tubes were centrifuged at 1500 r/min for 15 min. The absorbance of the supernatant was measured at 540 nm. Deionized water and normal saline were set as positive and negative groups respectively. The hemolysis rate was calculated according to formula (5):

$$\text{Hemolysis}(\%) \frac{OD_s - OD_n}{OD_p - OD_n} \times 100\% \quad (4)$$

OD_S is the absorbance of sponge or gauze. OD_n represents the absorbance of sterile saline and OD_p means the absorbance of deionized water.

Blood Clotting Index

BCI measurement was based on the previous study (Wu et al., 2020). 100 μL $CaCl_2$ (0.1 M) was added into 1 ml anticoagulant rabbit blood to activate blood. Then, 50 μL activated blood was immediately added into 10 mg sponge and incubated at 37°C for 30, 60, 90, and 120 s, respectively. Next 10 ml deionized water was added at the end of each time point and incubated at 37°C for 5 min. Finally, the absorbance was measured at 540 nm. The experiment was repeated 3 times. The gauze was set as the control group. The Blood Clotting Index (BCI) was calculated by formula (6):

$$BCI = [A_s - A_d / A_n - A_d] \times 100\% \quad (5)$$

"As" is the absorbance of sponges or gauze; "An" and "A_d" is the absorbance of the negative group and deionized water respectively.

The Evaluation of Biocompatibility

The sponge was irradiated under an ultraviolet lamp for 30 min to sterilize. After sterilization, the sponges were soaked in a cell culture medium for 24 h and then discarded and the culture medium was filtered with a 0.22 μm filter. The sponges were stored in a refrigerator at 4°C. A measure of 100 μL NIH-3T3 cell suspension with the concentration of 1×10^4 cells/mL was added to each well in 96 well-plate and cultured in a cell incubator for 12 h. After removing the supernatant, the sponge extract liquid (200 μg/ml) was added to a plate and cultured in a 37°C CO_2 incubator. The extracted liquid was changed every two days. On the days 1 and 3, the extract was removed and washed with PBS several times. 10 μL CCK-8 kit was added to each well and incubated in an incubator for 3 h. The OD value is measured at 450 nm. Cell proliferation rate is based on formula (7):

$$\text{Cell proliferation rate}\ (\%) = [A_s - A_b / A_c - A_b] \times 100\% \quad (6)$$

"A_s" is the absorbance of sponge extract; "A_c" and "A_b"represented the absorbance of the control group and blank group respectively.

NIH-3T3 cells (5×10^4 cells/mL) were added to the 24-well plate and incubated in the cell incubator for 1 day. Then, sponge extract solution was added and the extract solution was changed every two days. On days 1 and 3, the media was removed and cleaned with PBS 3 times. Finally, AO/EB reagent was added and incubated in a dark environment for 15 min. The cell morphology was observed with a fluorescence microscope.

Whole Blood Adhesion Test

The test method refers to the published literature (Liu et al., 2020; Fan et al., 2021). 100 μL anticoagulant rabbit blood was added to the surface of the sponge and activated at 37°C for 5 min. After being fixed with 2.5% glutaraldehyde for 2 h, the sponge was dehydrated in ethanol solution with concentration gradients (30,

50, 75, 95, and 100%) for 15 min. Then, the sponge was washed with PBS several times. Finally, the sponge was freeze-dried and the erythrocyte adhesion was observed by SEM.

In Vivo Hemostasis Test

In vivo hemostasis test of sponges was finished by tail experiment in mice and liver injury experiment in rats. The mice and rats were purchased from Qingdao Daren Fortune Animal Technology Co., Ltd., China. All animals were kept in a pathogen-free environment and fed ad lib. All animal experiments are approved by the Animal Ethics Committee of Shandong University and all applicable institutional and governmental regulations concerning the ethical use of animals were followed.

The mice (Kunming, male, 5–6 weeks, 35–40 g) were randomly divided into 5 groups. The tails of all mice were cut in half with a surgical scalpel. Then, the bleeding site was immediately covered with a sponge (W_1). The hemostatic time was recorded and the hemostatic material (W_2) was weighed to calculate the blood loss. The wound without treatment was set as a blank group and the wound treated with gauze was considered as the control group. After the experiment, the mice were killed by cervical dislocation.

The rats (SD, male, 7–8 weeks, 200–250 g) were anesthetized with 10% chloral hydrate and fixed on the surgical plate. The liver was exposed and injured with a biopsy instrument (diameter: 10 mm). The injury was immediately covered with sponge (W_1) and the hemostatic time was recorded. The sponge (W_2) after hemostasis was weighed to calculate blood loss. The wound covered with gauze was set as the control group and the wound without treatment was used as the blank group. After the experiment, the rats were killed by intraperitoneal injection of excessive chloral hydrate.

In Vivo Wound Healing Analysis

The rats (SD, male, 7–8 weeks, 200–250 g) were randomly divided into 5 groups. Then, the rats were anesthetized with 10% chloral hydrate and fixed on the board. Two round wounds with a diameter of 15 mm were fabricated on both sides of the back respectively. The wound was covered with sponge and photograped on days 0, 7, and 14. On days 7 and 14, the wound site was collected and H&E and Masson staining were used to further study the recovery. The rats were purchased from the DaRenFuCheng Experimental Animal Service Department of QingDao, China. After the experiment, the rats were killed by intraperitoneal injection of excessive chloral hydrate. All animal experiments are approved by the Animal Ethics Committee of Shandong University and all applicable institutional and governmental regulations concerning the ethical use of animals were followed.

Statistical Analysis

The results were expressed as means ± SDs. GraphPad Prism was used for analysis, one-way analysis of variance was used for comparison of results, and *t*-test was used for pial comparison between treatments. $p^* < 0.05$, $p^{**} < 0.01$ and $p^{***} < 0.001$ was considered as statistically significant.

RESULTS AND DISCUSSION

Preparation of CMC/CMCS-PDA

Scheme 1 shows the fabrication process of the CMC/CMCS-PDA sponge, which includes two times crosslinking and freeze-drying. First, DA crosslinks with CMCS and finishes polymerization to form CMCS-PDA structure through Michael addition reaction. Next, CMC is linked by CMCS-PDA with cross-linking agent EDC/NHS. The CMC/CMCS-PDA sponge is prepared after freeze-drying. The sponges are expected to be applied in wound hemostasis and repair.

Surface Morphology and Physico-Chemical Properties

Figure 1A shows the pore structure of prepared CMC/PDA and CMC/CMCS-PDA sponges. With the increase of CMCS, the pore size gradually decreases, which is attributed to the increased cross-linking sites provided by CMCS. The intensity of crosslinking is enhanced with CMCS incorporation. **Figure 1B** is the photograph of CMC/PDA and CMC/CMCS-PDA sponges. The color of the prepared sponges is black, which shows the formation of PDA in the sponges. In order to further study the chemical group composition, the sponges were tested by infrared spectroscopy. **Figure 1C** shows that the in-plane C-H bending vibration peak appeared at 1411cm^{-1} of CMC/PDA and CMC/CMCS-PDA, and the absorption peak of CMC/CMCS-PDA is stronger than that of CMC/PDA, which is caused by the introduction of CMCS. At 1597cm^{-1}, the stretching vibration of C=O and N-H bending vibration of amide II appear, indicating the formation of an amide bond. The C-N stretching vibration peak of amide III appeared at 1316cm^{-1}, and the absorption peak of CMC/CMCS-PDA is significantly stronger than CMC/PDA, suggesting that CMCS-PDA formed through the Michael addition reaction. Further degradability tests were carried out on the four groups of prepared sponges. **Figure 1D** shows that CMC/PDA sponges degrade rapidly and dissolve within 1 day. The interaction of each component in the CMC/PDA sponge is mainly provided by hydrogen bonds, which leads to unstable performance in PBS. At the same time, the stability of the CMC/CMCS-PDA sponge is gradually improved with the increasing dosage of CMCS. The CMC/CMCS-PDA$_2$ sponge degrades by about 75% after 14 days, which is suitable for wound repair. **Figure 1E** shows that all the sponges prepared have good blood absorption ability. CMC/CMCS-PDA has better blood absorption ability than CMC/PDA and its stable structure enables the sponge to better fix blood. **Figure 1F** shows the swelling rate of CMC/PDA and CMC/CMCS-PDA sponges. CMC/PDA sponge disperses quickly in PBS solution, which does not meet the requirements of use. The prepared CMC/CMCS-PDA has a stable swelling rate and still keeps stable after absorbing enough water.

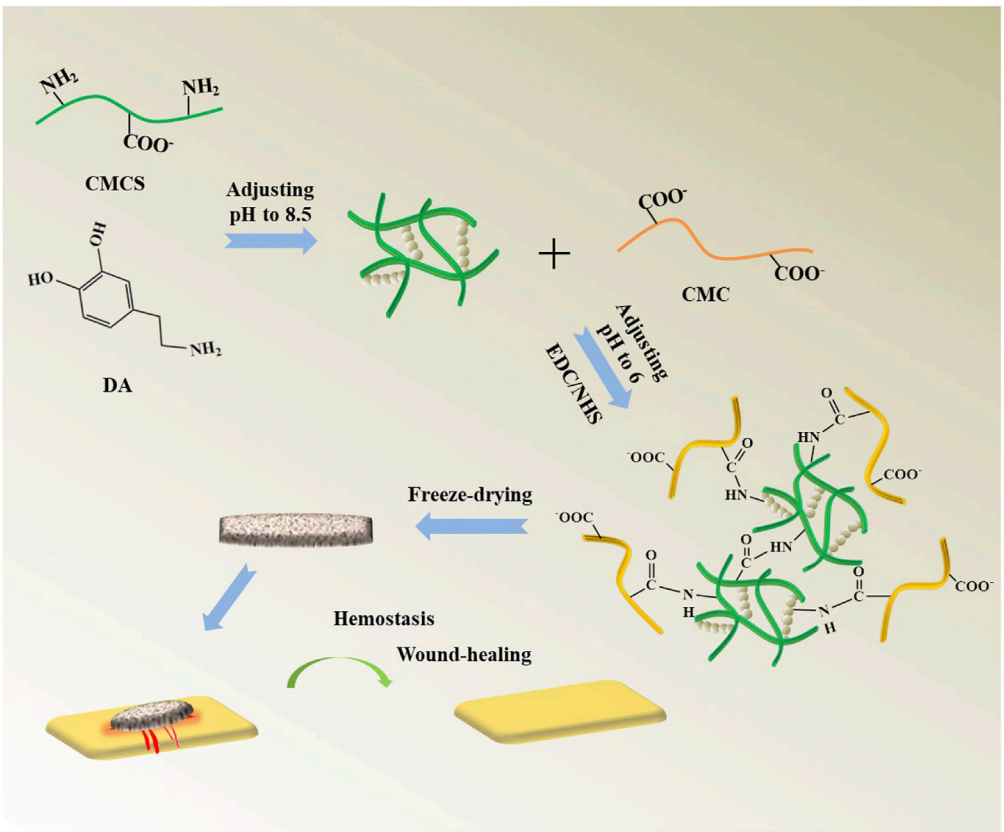

SCHEME 1 | Fabrication process of the CMC/CMCS-PDA sponge and its application to hemostasis and wound repair.

Antibacterial Properties

The good antibacterial properties of sponges can help reduce infection at wound sites (Bayon et al., 2018; Chen et al., 2018; Liu et al., 2021b). The antibacterial activity of CMC/PDA and CMC/CMCS-PDA sponges was investigated by the colony formation method. **Figure 2A** shows the test process of the sponge on inhibiting bacterial growth in a liquid medium. **Figure 2B** is the absorbance of liquid medium containing sponge after culturing with bacteria for 4 h. CMC/PDA and CMC/CMCS-PDA sponges all have inhibitory effects on the growth of *E. coli* and *S. aureus*. CMC/CMCS-PDA sponge has an obvious inhibitory effect on bacteria growth. In addition, CMC/CMCS-PDA_2 and CMC/CMCS-PDA_3 have best antibacterial activity.

Hemostatic Performance

In order to further study the blood cells adhesion on the prepared sponges, the blood cells adhesion was observed by SEM (**Figure 3A**). Compared with the gauze group, the blood cells on CMC/PDA sponge significantly increase and the blood cells' adhesion of CMC/CMCS-PDA group is further improved. There is no significant difference between the three CMC/CMCS-PDA groups, which is due to the stable pore structure of the CMC/CMCS-PDA sponge. **Figure 3B** is a tail-cutting model in mice. According to the blood loss in **Figure 3C**, the hemostatic effect of CMC/PDA and CMC/CMCS-PDA sponge is significantly stronger than that of gauze, and the hemostatic effect of CMC/CMCS-PDA_2 and CMC/CMCS-PDA_3 is significantly higher than that of CMC/PDA. The stability of the sponge can maintain the structure of the sponge and enhance the hemostatic ability. The blood clotting index (BCI) of the prepared sponge is further investigated. **Figure 3D** shows that CMC/PDA has better coagulation ability than gauze. With the increase of time, the coagulation effect of each group gradually increases. Compared with gauze and CMC/PDA sponges and CMC/CMCS-PDA sponges can achieve rapid blood coagulation, among which CMC/CMCS-PDA_2 sponge has the fastest coagulation speed. The appropriate incorporation of CMCS endows CMC/CMCS-PDA sponge's stable structure and hemostatic potential. **Figure 3E** is a rat liver injury model. The results of **Figure 3F** and **Figure 3G** show that the hemostatic effect and hemostatic time of the CMC/PDA sponge are better than that of gauze. The blood loss and hemostatic time of CMC/CMCS-PDA are further reduced, while CMC/CMCS-PDA2 showed the best hemostatic effect, which further illustrates that a stable sponge structure can promote hemostatic effect.

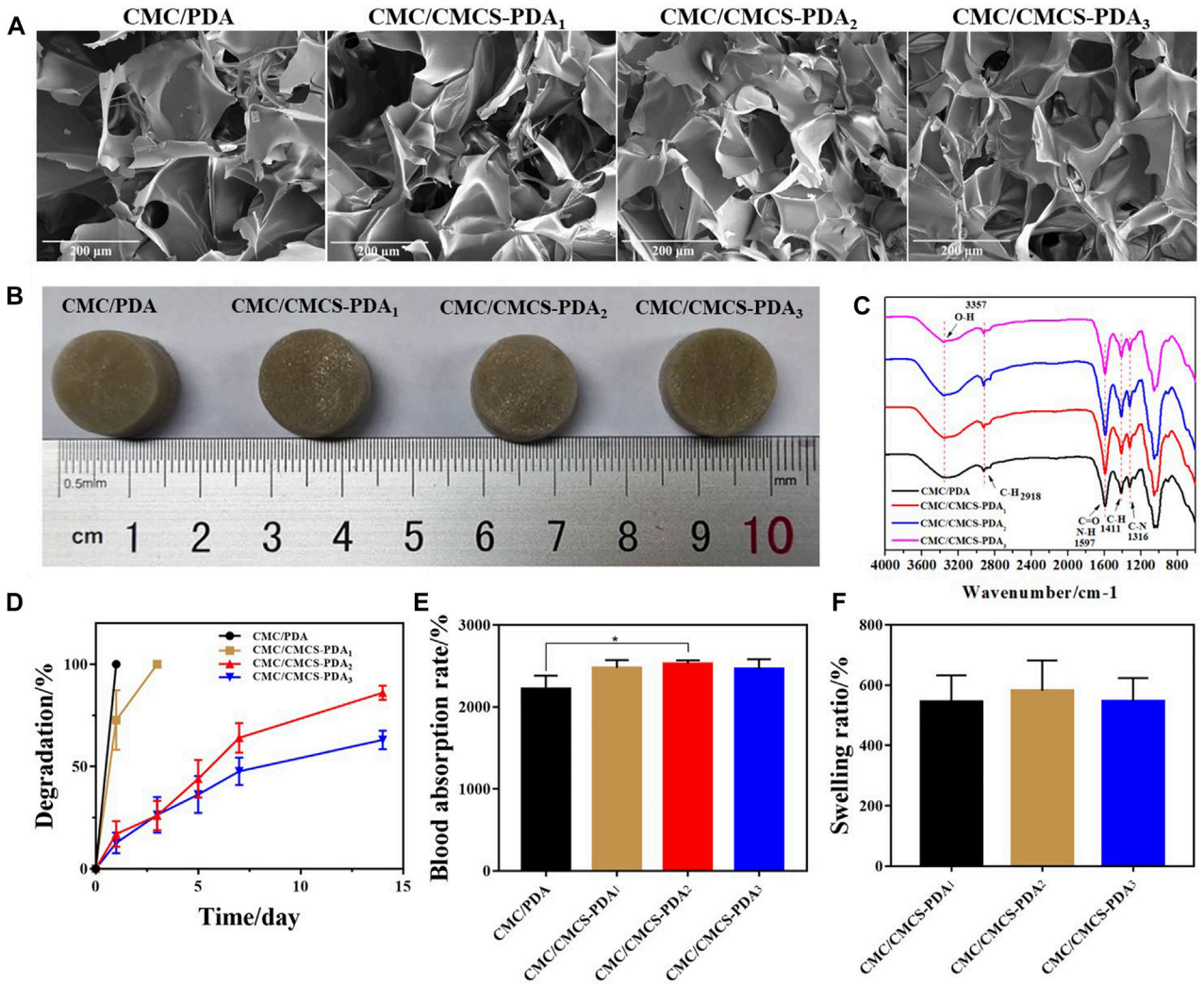

FIGURE 1 | (A) SEM images of CMC/PDA and CMC/CMCS-PDA sponges. **(B)** Photographs of prepared CMC/PDA and CMC/CMCS-PDA sponges. **(C)** FTIR spectra of CMC/PDA and CMC/CMCS-PDA sponges. **(D)** Degradation, **(E)** blood absorption rate, and **(F)** swelling rate of prepared CMC/PDA and CMC/CMCS-PDA sponges.

In Vitro and *In Vivo* Biocompatibility

The biocompatibility of the sponges was further tested. NIH-3T3 cells were co-cultured with sponge extract for 3 days and the cell growth was observed by AO/EB staining. **Figure 4A** shows that after 3 days of culture, the number of cells further increases, and the cell morphology of prepared CMC/PDA and CMC/CMCS-PDA is normal. The proliferation of NIH-3T3 cells was studied by the CCK-8 proliferation test. As shown in **Figure 4B**, compared with the blank group, cell proliferation increases in CMC/PDA and CMC/CMCS-PDA groups on the first day. After 3 days of culturing, cell proliferation is more obvious than that of the blank group, but there is no significant difference between the CMC/PDA and CMC/CMCS-PDA groups, which could due to the similar components of CMC/PDA and CMC/CMCS-PDA. Both CMC/PDA and CMC/CMCS-PDA can promote the proliferation of NIH-3T3 cells. Following, the free radical scavenging ability of CMC/PDA and CMC/CMCS-PDA sponges was tested. **Figure 4C** shows the contrast images of free radical scavenging. CMC/PDA group becomes lighter in color compared with the blank group and the color in CMC/CMCS-PDA group further reduces, which indicates that CMC/CMCS-PDA has a stronger scavenging ability than CMC/PDA. ABTS free radical scavenging results in **Figure 4D** show that the free radical scavenging ability of the CMC/PDA sponge is only about 15%, while CMC/CMCS-PDA groups reach about 40%, which is due to the high solubility of CMC/PDA. The aqueous solution mixed with PDA in the extraction process is difficult to be separated from the CMC/PDA sponge, leading to the low concentration of PDA in the supersuperant. Good free radical scavenging ability can reduce the inflammatory reaction of the wound site and promote healing (Xu et al., 2020; Tamer et al., 2021). **Figure 4E** shows the hemolysis rates of prepared sponges. The hemolysis

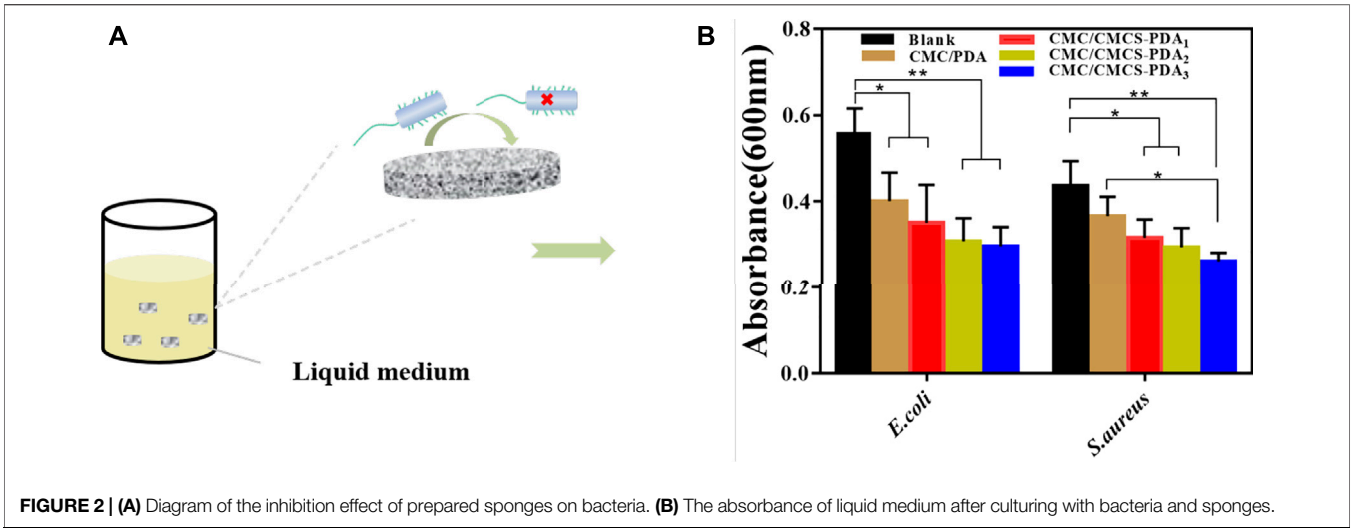

FIGURE 2 | (A) Diagram of the inhibition effect of prepared sponges on bacteria. **(B)** The absorbance of liquid medium after culturing with bacteria and sponges.

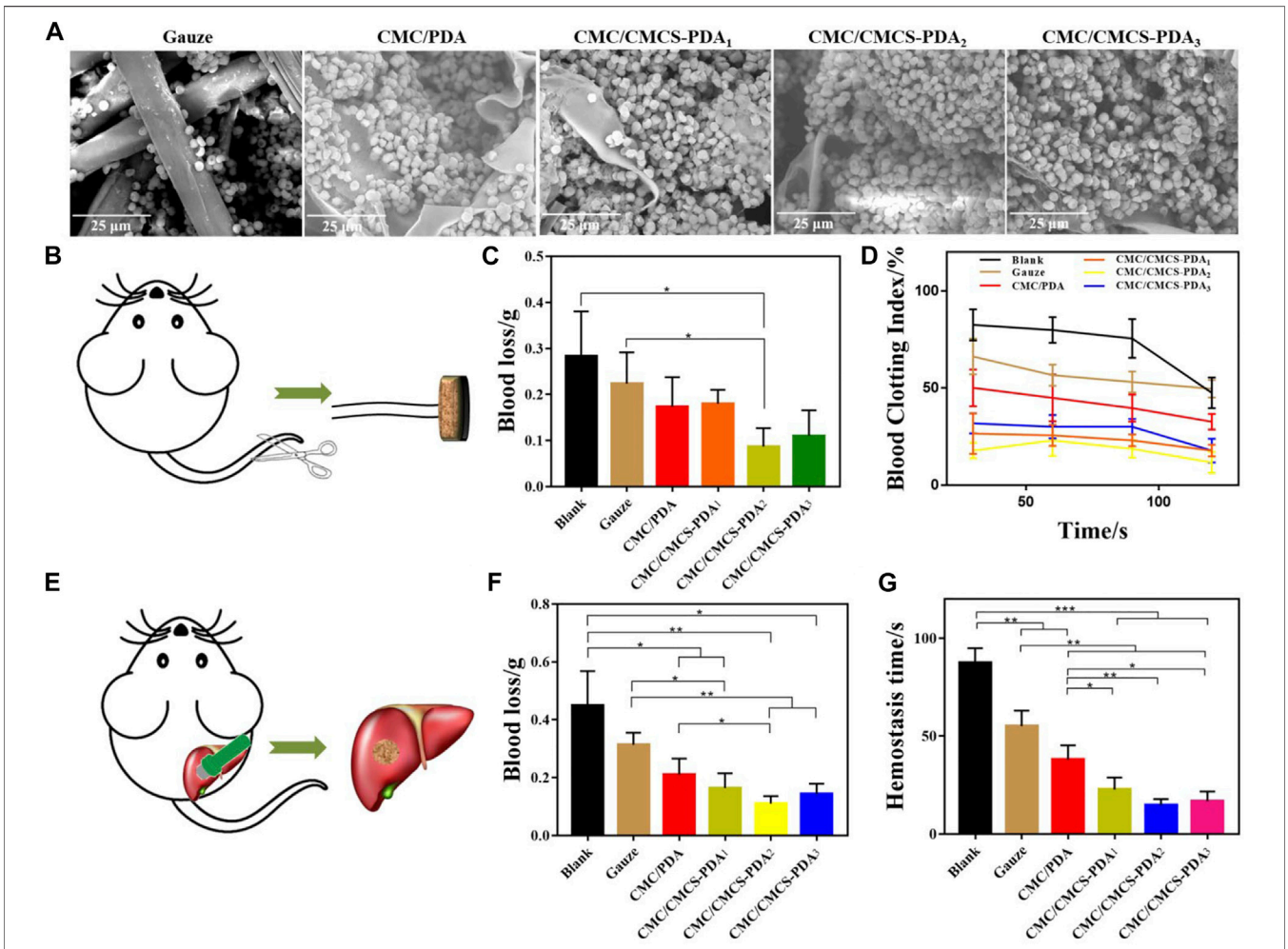

FIGURE 3 | (A) SEM images of hemocyte adhesion of gauze, CMC/PDA, and CMC/CMCS-PDA sponges. **(B)** Tail cutting process in mice. **(C)** The blood loss of mice in tail cutting treated with gauze, CMC/PDA, and CMC/CMCS-PDA sponges. **(D)** Blood clotting index test of gauze, CMC/PDA, and CMC/CMCS-PDA sponges. **(E)** The building process of rat liver injury model. **(F)** Blood loss and **(G)** hemostasis time of rat liver injury treated with gauze, CMC/PDA, and CMC/CMCS-PDA sponges.

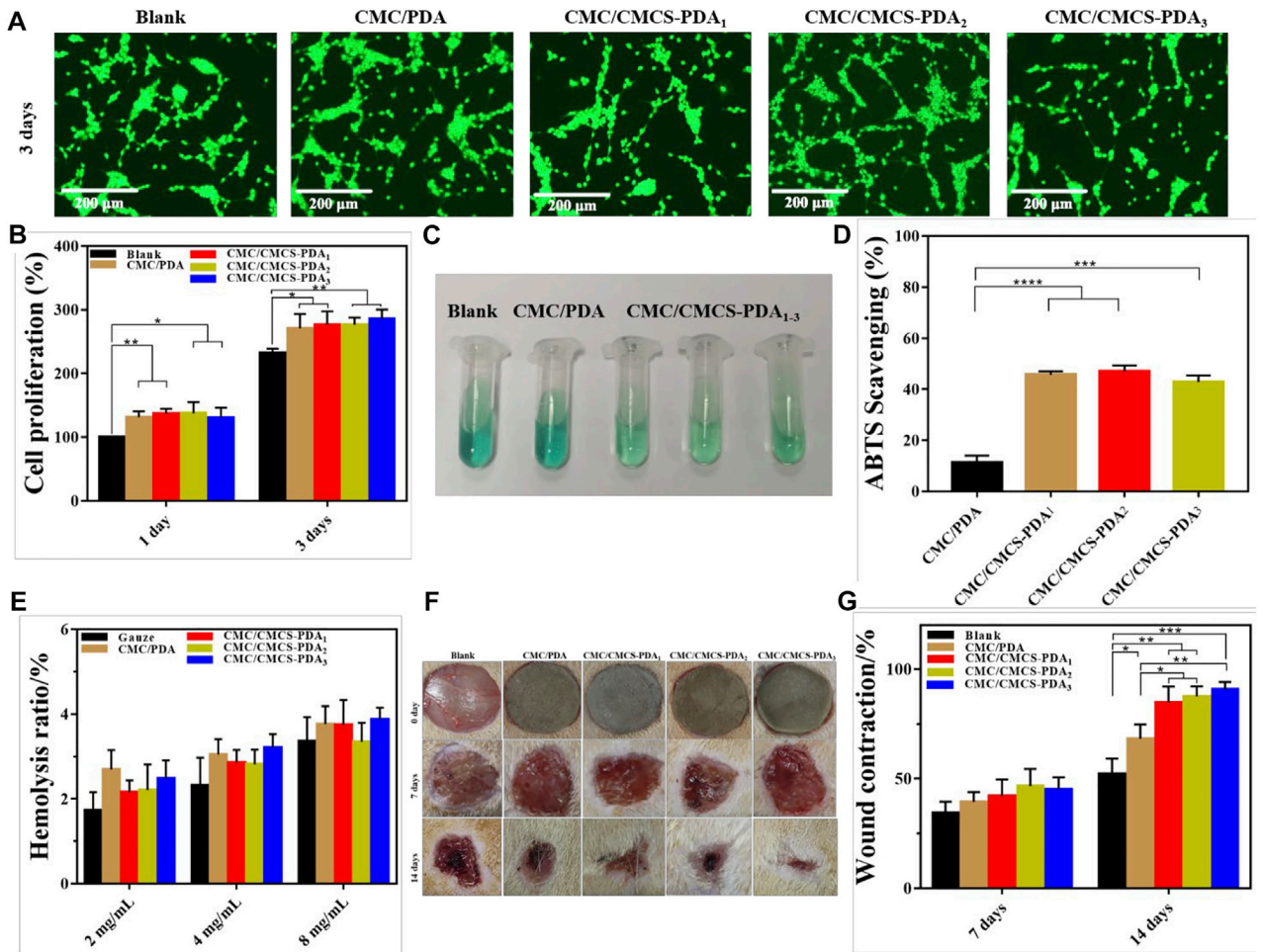

FIGURE 4 | (A) AO/EB staining of NIH-3T3 cell after co-culturing with extract liquid of CMC/PDA and CMC/CMCS-PDA sponges. **(B)** CCK-8 NIH-3T3 cell proliferation tests after co-culturing with extract liquid of CMC/PDA and CMC/CMCS-PDA sponges for 1 and 3 days. **(C)** Photograph of ABTS radicals scavenging and **(D)** results of radicals scavenging. **(E)** Hemolysis ratio of CMC/PDA and CMC/CMCS-PDA sponges at a concentration of 2, 4, and 8 mg/ml. **(F)** Photographs of wound site in rat at days of 0, 7, and 14. **(G)** The results of wound contraction at days 7 and 14.

rate of each group is lower than 5% at 4 mg/ml, which met the international standard. When the concentration reached 8 mg/ml, the hemolysis rates of CMC/PDA and CMC/CMCS-PDA_1 are both higher than 5% for their poor stability. However, CMC/CMCS-PDA_2 and CMC/CMCS-PDA_3 still meet the requirements. Further *in vivo* study on wound repair of sponges (**Figure 4F**) shows that CMC/CMCS-PDA_2 and CMC/CMCS-PDA_3 sponges have the best repair on days 7. At day 14, CMC/PDA and CMC/CMCS-PDA groups show obvious repair effect compared with the blank group, and CMC/CMCS-PDA_2 and CMC/CMCS-PDA_3 still have the best repair effect, which is related to the stable structure of CMC/CMCS-PDA_2 and CMC/CMCS-PDA_3 sponges. According to the calculation of the wound repair area in **Figure 4G**, the results further confirmed that CMC/CMCS-PDA_2 and CMC/CMCS-PDA_3 groups have the best repair effect at days 7 and 14.

Histological Staining Analysis

Figure 5A shows the HE staining of cross sections at rat wound site at days 7 and 14. On day 7, sparse tissue is observed in the blank group, while the new tissue in CMC/PDA and CMC/CMCS-PDA groups is denser. Compared with CMC/CMCS-PDA group, there are more inflammatory cells in the CMC/PDA group, which is related to the instability of the sponge *in vivo*. After 14 days, collagen tissue formation is more abundant in the blank group. Compared with the blank group, the collagen tissues in CMC/PDA group arrange neatly. In the CMC/CMCS-PDA group, tissue formation is complete and the hair follicles have appeared on the surrounding skin. **Figure 5B** shows the Masson staining of cross sections at the wound site. On day 7, collagen fibers are sparse in the blank group, while arranged collagen fibers can be observed in CMC/PDA group. The collagen fibers in CMC/CMCS-PDA arrange neatly and the tissue formation is complete. On day

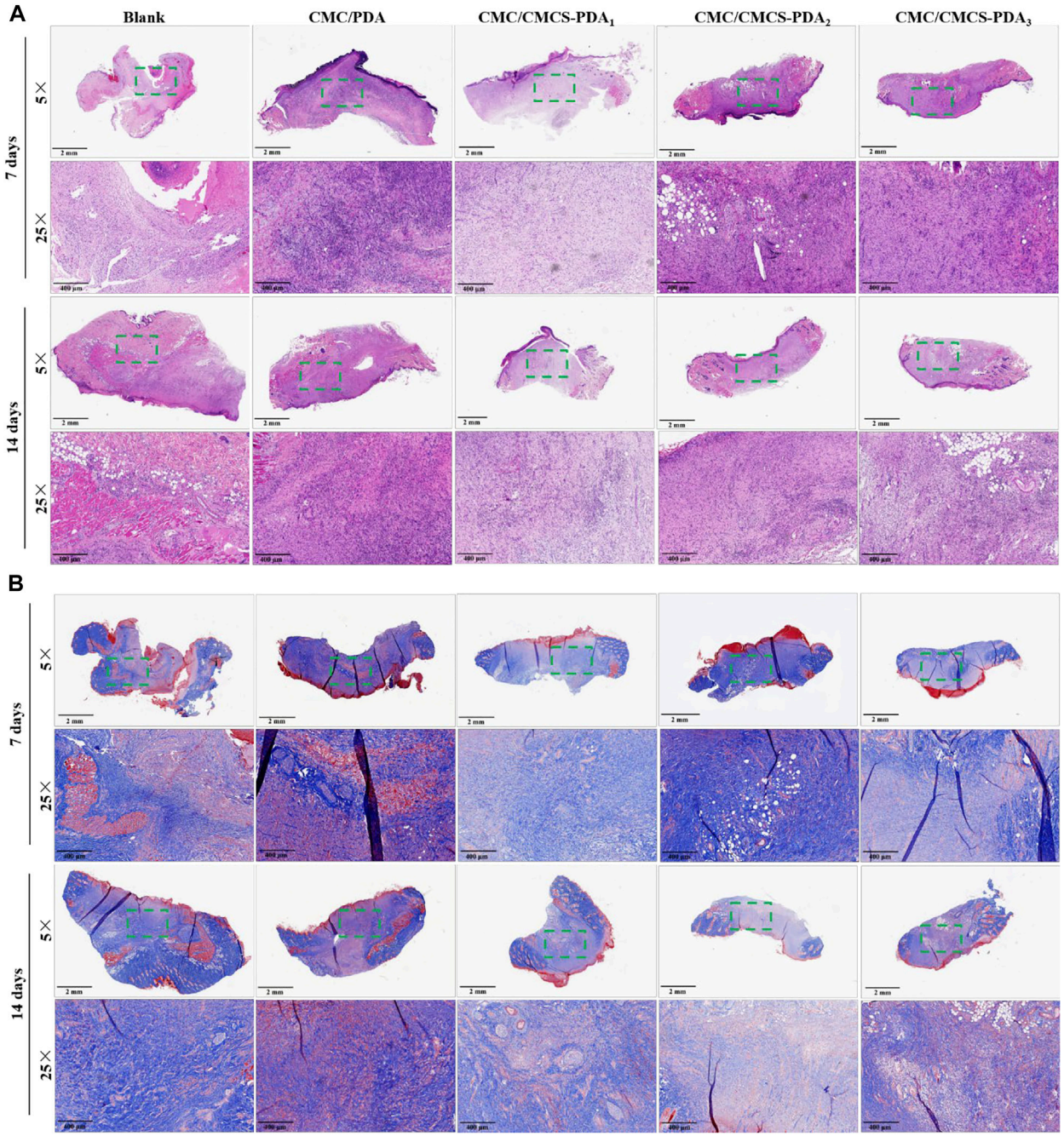

FIGURE 5 | (A) H&E staining of wound site at cross sections of control, CMC/PDA, and CMC/CMCS-PDA groups on day 7. **(B)** Masson staining of wound site at cross sections of control, CMC/PDA, and CMC/CMCS-PDA groups on day 14.

14, in the blank group, collagen fibers form densely while muscle fibers only appear partly. Collagen fibers and muscle fibers evenly distribute in CMC/PDA group. In CMC/CMCS-PDA group, collagen fibers and muscle fibers arrange neatly and hair follicle formation can be observed. Combined with the wound closure area, CMC/CMCS-PDA_2 and CMC/CMCS-PDA_3 sponges have the best promoting effect on wound repair.

CONCLUSION

In summary, dopamine auto-polymerizes and cross-links with CMCS through the Michael addition reaction to form CMCS-PDA structure. CMC/CMCS-PDA sponge was obtained by cross-linking CMC with CMCS-PDA. By adjusting the amount of CMCS, the stability of the CMC/CMCS-PDA sponge was investigated. The results show that the stability of the CMC/CMCS-PDA sponge was

improved gradually with the increase of CMCS. Meanwhile, the introduction of CMCS-PDA improved the hemostatic and antibacterial properties of the CMC sponge. CMC/CMCS-PDA_2 has the best hemostatic effect in the rat liver injury model and mouse tail severing experiment for its appropriate cross-linking degree. The biocompatibility tests show that CMC/CMCS-PDA sponge can better promote the proliferation of NIH-3T3 cells than the blank group and CMC/PDA. Further rat skin defect models showed that CMC/CMCS-PDA_2 and CMC/CMCS-PDA_3 group has the best repair effect. Above, we conclude that CMC/CMCS-PDA_2 sponge has great potential in wound repair and hemostasis.

DATA AVAILABILITY STATEMENT

The original contributions presented in the study are included in the article/Supplementary materials, further inquiries can be directed to the corresponding author.

ETHICS STATEMENT

The animal study was reviewed and approved by Weihai Municipal Hospital Ethics Committee.

AUTHOR CONTRIBUTIONS

ZB: Methodology, Data curation, Formal analysis, Writing—original draft. HT: Investigation, Data curation QL: Writing—review and editing. SZ: Resources, Project administration, Funding acquisition.

FUNDING

This work was supported by the National Natural Science Fund (No. 81560123).

REFERENCES

Bayon, B., Cacicedo, M. L., Alvarez, V. A., and Castro, G. R. (2018). Self-assembly stereo-specific synthesis of silver phosphate microparticles on bacterial cellulose membrane surface for antimicrobial applications. *Colloid Interface Sci. Commun.* 26, 7–13. doi:10.1016/j.colcom.2018.07.002

Beck, G. C., Brinkkoetter, P., Hanusch, C., Schulte, J., van Ackern, K., van der Woude, F. J., et al. (2004). Clinical review: Immunomodulatory effects of dopamine in general inflammation. *Crit. Care* 8, 485–491. doi:10.1186/cc2879

Buraczewska, I., Brostrom, U., and Loden, M. (2007). Artificial reduction in transepidermal water loss improves skin barrier function. *Br. J. Dermatol.* 157, 82–86. doi:10.1111/j.1365-2133.2007.07965.x

Chang, C. Y., and Zhang, L. N. (2011). Cellulose-based hydrogels: Present status and application prospects. *Carbohydr. Polym.* 84, 40–53. doi:10.1016/j.carbpol.2010.12.023

Chen, H. L., Lan, G. Q., Ran, L. X., Xiao, Y., Yu, K., Lu, B. T., et al. (2018). A novel wound dressing based on a Konjac glucomannan/silver nanoparticle composite sponge effectively kills bacteria and accelerates wound healing. *Carbohydr. Polym.* 183, 70–80. doi:10.1016/j.carbpol.2017.11.029

Cheng, H. H., Xiong, J., Xie, Z. N., Zhu, Y. T., Liu, Y. M., Wu, Z. Y., et al. (2018). Thrombin-Loaded poly(butylene succinate)-based electrospun membranes for rapid hemostatic application. *Macromol. Mat. Eng.* 303, 1700395. doi:10.1002/mame.201700395

Cheng, H., Li, C. J., Jiang, Y. J., Wang, B. J., Wang, F. J., Mao, Z. P., et al. (2018). Facile preparation of polysaccharide-based sponges and their potential application in wound dressing. *J. Mat. Chem. B* 6, 634–640. doi:10.1039/c7tb03000b

Diaz-Gomez, L., Gonzalez-Prada, I., Millan, R., Da Silva-Candal, A., Bugallo-Casal, A., Campos, F., et al. (2022). 3D printed carboxymethyl cellulose scaffolds for autologous growth factors delivery in wound healing. *Carbohydr. Polym.* 278, 118924. doi:10.1016/j.carbpol.2021.118924

Eivazzadeh-Keihan, R., Khalili, F., Khosropour, N., Aliabadi, H. A. M., Radinekiyan, F., Sukhtezari, S., et al. (2021). Hybrid bionanocomposite containing magnesium hydroxide nanoparticles embedded in a carboxymethyl cellulose hydrogel plus silk fibroin as a scaffold for wound dressing applications. *ACS Appl. Mat. Interfaces* 13, 33840–33849. doi:10.1021/acsami.1c07285

Fan, X. L., Li, M. Y., Yang, Q., Wan, G. M., Li, Y. J., Li, N., et al. (2021). Morphology-controllable cellulose/chitosan sponge for deep wound hemostasis with surfactant and pore-foaming agent. *Mater. Sci. Eng. C* 118, 111408. doi:10.1016/j.msec.2020.111408

Faure, E., Falentin-Daudré, C., Jérôme, C., Lyskawa, J., Fournier, D., Woisel, P., et al. (2013). Catechols as versatile platforms in polymer chemistry. *Prog. Polym. Sci.* 38, 236–270. doi:10.1016/j.progpolymsci.2012.06.004

Felger, J. C., and Miller, A. H. (2012). Cytokine effects on the basal ganglia and dopamine function: The subcortical source of inflammatory malaise. *Front. Neuroendocrinol.* 33, 315–327. doi:10.1016/j.yfrne.2012.09.003

Ghomi, E. R., Khalili, S., Khorasani, S. N., Neisiany, R. E., and Ramakrishna, S. (2019). Wound dressings: Current advances and future directions. *J. Appl. Polym. Sci.* 136, 47738. doi:10.1002/app.47738

Gurtner, G. C., Werner, S., Barrandon, Y., and Longaker, M. T. (2008). Wound repair and regeneration. *Nature* 453, 314–321. doi:10.1038/nature07039

Halib, N., Perrone, F., Cemazar, M., Dapas, B., Farra, R., Abrami, M., et al. (2017). Potential applications of nanocellulose-containing materials in the biomedical field. *Materials* 10, 977. doi:10.3390/ma10080977

Han, W., Zhou, B., Yang, K., Xiong, X., Luan, S. F., Wang, Y., et al. (2020). Biofilm-inspired adhesive and antibacterial hydrogel with tough tissue integration performance for sealing hemostasis and wound healing. *Bioact. Mater.* 5, 768–778. doi:10.1016/j.bioactmat.2020.05.008

Kanikireddy, V., Varaprasad, K., Jayaramudu, T., Karthikeyan, C., and Sadiku, R. (2020). Carboxymethyl cellulose-based materials for infection control and wound healing: A review. *Int. J. Biol. Macromol.* 164, 963–975. doi:10.1016/j.ijbiomac.2020.07.160

Khalf-Alla, P. A., Basta, A. H., Lotfy, V. F., and Hassan, S. S. (2021). Synthesis, characterization, speciation, and biological studies on metal chelates of carbohydrates with molecular docking investigation. *Macromol. Mat. Eng.* 306, 2000633. doi:10.1002/mame.202000633

Li, M., Zhang, Z., Liang, Y., He, J., and Guo, B. (2020). Multifunctional tissue-adhesive cryogel wound dressing for rapid nonpressing surface hemorrhage and wound repair. *ACS Appl. Mat. Interfaces* 12, 35856–35872. doi:10.1021/acsami.0c08285

Liang, W. C., Lu, Q. H., Yu, F., Zhang, J. Y., Xiao, C., Dou, X. M., et al. (2021). A multifunctional green antibacterial rapid hemostasis composite wound dressing for wound healing. *Biomater. Sci.* 9, 7124–7133. doi:10.1039/d1bm01185e

Lin, P. J., Liu, L. L., He, G. H., Zhang, T., Yang, M., Cai, J. Z., et al. (2020). Preparation and properties of carboxymethyl chitosan/oxidized hydroxyethyl cellulose hydrogel. *Int. J. Biol. Macromol.* 162, 1692–1698. doi:10.1016/j.ijbiomac.2020.07.282

Liu, C. Y., Liu, C. Y., Yu, S. M., Wang, N., Yao, W. H., Liu, X., et al. (2020). Efficient antibacterial dextran-montmorillonite composite sponge for rapid hemostasis with wound healing. *Int. J. Biol. Macromol.* 160, 1130–1143. doi:10.1016/j.ijbiomac.2020.05.140

Liu, F. F., Liu, X., Chen, F., and Fu, Q. (2021). Mussel-inspired chemistry: A promising strategy for natural polysaccharides in biomedical applications. *Prog. Polym. Sci.* 123, 101472. doi:10.1016/j.progpolymsci.2021.101472

Liu, W. S., Yang, C. F., Gao, R., Zhang, C., Ou-Yang, W. B., Feng, Z. J., et al. (2021). Polymer composite sponges with inherent antibacterial, hemostatic, inflammation-modulating and proregenerative performances for methicillin-resistant Staphylococcus aureus-infected wound healing. *Adv. Healthc. Mat.* 10, 2201394. doi:10.1002/adhm.202201394

Liu, Y., Chen, Y., Zhao, Y., Tong, Z. R., and Chen, S. S. (2015). Superabsorbent sponge and membrane prepared by polyelectrolyte complexation of carboxymethyl cellulose/hydroxyethyl cellulose-Al3+. *Bioresources* 10, 6479–6495. doi:10.15376/biores.10.4.6479-6495

Nelson, C., Tuladhar, S., Launen, L., and Habib, A. (1800). 3D bio-printability of hybrid pre-crosslinked hydrogels. *Int. J. Mol. Sci.* 22, 13481. doi:10.3390/ijms222413481

Ohta, S., Mitsuhashi, K., Chandel, A. K. S., Qi, P., Nakamura, N., Nakamichi, A., et al. (2022). Silver-loaded carboxymethyl cellulose nonwoven sheet with controlled counterions for infected wound healing. *Carbohydr. Polym.* 286, 119289. doi:10.1016/j.carbpol.2022.119289

Ong, S. Y., Wu, J., Moochhala, S. M., Tan, M. H., and Lu, J. (2008). Development of a chitosan-based wound dressing with improved hemostatic and antimicrobial properties. *Biomaterials* 29, 4323–4332. doi:10.1016/j.biomaterials.2008.07.034

Park, J. U., Song, E. H., Jeong, S. H., Song, J., Kim, H. E., and Kim, S. (2018). "Chitosan-based dressing materials for problematic wound management," in *Novel biomaterials for regenerative medicine*. Editors H. J. Chun, K. Park, C. H. Kim, and G. Khang, 527–537.

Pei, Y., Ye, D. D., Zhao, Q., Wang, X. Y., Zhang, C., Huang, W. H., et al. (2015). Effectively promoting wound healing with cellulose/gelatin sponges constructed directly from a cellulose solution. *J. Mat. Chem. B* 3, 7518–7528. doi:10.1039/c5tb00477b

Peng, S., Liu, W., Han, B., Chang, J., Li, M., and Zhi, X. (2011). Effects of carboxymethyl-chitosan on wound healing *in vivo* and *in vitro*. *J. Ocean. Univ. China* 10, 369–378. doi:10.1007/s11802-011-1764-y

Pettignano, A., Charlot, A., and Fleury, E. (2019). Carboxyl-functionalized derivatives of carboxymethyl cellulose: Towards advanced biomedical applications. *Polym. Rev.* 59, 510–560. doi:10.1080/15583724.2019.1579226

Pinpru, N., and Woramongkolchai, S. (2020). Crosslinking effects on alginate/carboxymethyl cellulose packaging film properties. *Chiang Mai J. Sci.* 47, 712–722.

Qiu, W. Z., Wu, G. P., and Xu, Z. K. (2018). Robust coatings *via* catechol-amine codeposition: Mechanism, kinetics, and application. *ACS Appl. Mat. Interfaces* 10, 5902–5908. doi:10.1021/acsami.7b18934

Saporito, F., Sandri, G., Rossi, S., Bonferoni, M. C., Riva, F., Malavasi, L., et al. (2018). Freeze dried chitosan acetate dressings with glycosaminoglycans and traxenamic acid. *Carbohydr. Polym.* 184, 408–417. doi:10.1016/j.carbpol.2017.12.066

Saruchi and Kumar, V. (2020). Effective degradation of rhodamine B and Congo red dyes over biosynthesized silver nanoparticles-imbibed carboxymethyl cellulose hydrogel. *Polym. Bull. Berl.* 77, 3349–3365. doi:10.1007/s00289-019-02920-x

Tamer, T. M., Alsehli, M. H., Omer, A. M., Afifi, T. H., Sabet, M. M., Mohy-Eldin, M. S., et al. (2021). Development of polyvinyl alcohol/kaolin sponges stimulated by marjoram as hemostatic, antibacterial, and antioxidant dressings for wound healing promotion. *Int. J. Mol. Sci.* 22, 13050. doi:10.3390/ijms222313050

Upadhyaya, L., Singh, J., Agarwal, V., and Tewari, R. P. (2013). Biomedical applications of carboxymethyl chitosans. *Carbohydr. Polym.* 91, 452–466. doi:10.1016/j.carbpol.2012.07.076

Wang, S., Pi, L. L., Wen, H. Y., Yu, H., and Yang, X. G. (2020). Evaluation of novel magnetic targeting microspheres loading adriamycin based on carboxymethyl chitosan. *J. Drug Deliv. Sci. Technol.* 55, 101388. doi:10.1016/j.jddst.2019.101388

Wu, Z. G., Zhou, W., Deng, W. J., Xu, C. L., Cai, Y., and Wang, X. Y. (2020). Antibacterial and hemostatic thiol-modified chitosan-immobilized AgNPs composite sponges. *ACS Appl. Mat. Interfaces* 12, 20307–20320. doi:10.1021/acsami.0c05430

Xu, Z. J., Han, S. Y., Gu, Z. P., and Wu, J. (2020). Advances and impact of antioxidant hydrogel in chronic wound healing. *Adv. Healthc. Mat.* 9, 1901502. doi:10.1002/adhm.201901502

Yang, J., Cohen Stuart, M. A., and Kamperman, M. (2014). Jack of all trades: Versatile catechol crosslinking mechanisms. *Chem. Soc. Rev.* 43, 8271–8298. doi:10.1039/c4cs00185k

Zennifer, A., Senthilvelan, P., Sethuraman, S., and Sundaramurthi, D. (2021). Key advances of carboxymethyl cellulose in tissue engineering & 3D bioprinting applications. *Carbohydr. Polym.* 256, 117561. doi:10.1016/j.carbpol.2020.117561

Zhang, Y. P., Wang, Y., Chen, L., Zheng, J., Fan, X. J., Xu, X. L., et al. (2022). An injectable antibacterial chitosan-based cryogel with high absorbency and rapid shape recovery for noncompressible hemorrhage and wound healing. *Biomaterials* 285, 121546. doi:10.1016/j.biomaterials.2022.121546

Conflict of Interest: The authors declare that the research was conducted in the absence of any commercial or financial relationships that could be construed as a potential conflict of interest.

Publisher's Note: All claims expressed in this article are solely those of the authors and do not necessarily represent those of their affiliated organizations, or those of the publisher, the editors and the reviewers. Any product that may be evaluated in this article, or claim that may be made by its manufacturer, is not guaranteed or endorsed by the publisher.